CHEMICAL ENGINEERING TRANSACTIONS
VOL. 56, 2017
A publication of AIDIC
The Italian Association of Chemical Engineering
Online at www.aidic.it/cet
Guest Editors: Jiří Jaromír Klemeš, Peng Yen Liew, Wai Shin Ho, Jeng Shiun Lim

ISBN978-88-95608-47-1; **ISSN** 2283-9216
DOI: 10.3303/CET1756035

Achieving the Target Crystal Size Distribution in the Case of Agglomeration and Breakage for Batch Cooling Crystallisation Process

Zakirah Mohd Zahari, Suriyati Saleh, Noor Asma Fazli Abdul Samad*

Faculty of Chemical and Natural Resources Engineering, Universiti Malaysia Pahang, Lebuhraya Tun Razak, 26300 Gambang, Kuantan Pahang.
asmafazli@ump.edu.my

One of the main specification of crystallisation process is the crystal size distribution (CSD). In order to achieve the desired CSD, supersaturation or temperature control is applied to maintain the concentration or temperature at the required set-point trajectory which lies within the metastable zone. The set-point trajectory can be determined using the analytical CSD estimator where both the supersaturation/concentration set-point and batch time needed to achieve the desired target CSD can be estimated. The current analytical CSD estimator is applicable only for growth dominated phenomena and neglects the effects of agglomeration and breakage phenomena. Both phenomena occurs during crystallisation operation and may influences the CSD. Both agglomeration and breakage phenomena need to be considered during crystallisation operation in order to provide an accurate set-point trajectory and also to identify the effects of both phenomena on the performance of CSD. The objective of this work is to extend the analytical CSD estimator to cover the effects of agglomeration and breakage phenomena. Here the agglomeration and breakage phenomena are represented by kinetic power law equation and incorporated into the extended analytical CSD estimator. The application of this work is highlighted through a sucrose batch cooling crystallisation process case study where based on the identified target CSD, the extended analytical estimator is capable to generate the required set-point trajectory. The proposed controller is successfully maintained the operation at the desired set-point and achieving the target CSD in the case of agglomeration and breakage.

1. Introduction

Crystallisation is a solid-liquid separation process in which mass transfer of a solute from liquid solution to a pure solid crystalline phase occurs (Cristofer et al., 2011). It is one of the key unit operations which are commonly applied in the food, pharmaceutical and fine chemical industries (Ghadipasha et al., 2015). The specifications of the crystal product are usually measured in terms of crystal size, size distribution, shape and purity (Nagy and Braatz, 2012). In many crystallisation processes, the main problem is how to obtain a uniform and reproducible crystal size distribution (CSD) (Vetter et al., 2014). To overcome this problem, a supersaturation control or temperature control is one of the ways to control the distribution of crystal particles through batch cooling crystallisation process. For generating the set-point trajectory for the controller, analytical CSD estimator for predicting the set-point trajectory to achieve the desired CSD in batch cooling crystallisation has been developed by Samad et al. (2013). The current analytical CSD estimator is developed based on the assumptions of constant supersaturation throughout the entire batch operation and the growth dominated phenomena with the absence of nucleation. Through this estimator, the set-point trajectory which consists of supersaturation/concentration and total batch time is generated in order to obtain the target CSD. Subsequently supersaturation/concentration control is applied to drive the process at the desired set-point which usually lies within the metastable zone in order to enhance the control of the CSD. During the crystallisation operation, the crystal particles tend to merge or break through agglomeration and breakage phenomena due to the agitation effects. The CSD obtained in the end of the operation is affected by both phenomena. The objective of this paper is to extend the original analytical CSD estimator to cover the effects

Please cite this article as: Zahari Z.M., Saleh S., Samad N.A.F.A., 2017, Achieving the target crystal size distribution in the case of agglomeration and breakage for batch cooling crystallization process, Chemical Engineering Transactions, 56, 205-210
DOI:10.3303/CET1756035

of the agglomeration and breakage phenomena and analyse its influence on the final CSD. The application of the extended analytical CSD estimator is highlighted through sucrose batch cooling crystallisation case study where the set-point needed to achieve the desired target CSD is generated using this estimator. The performance of the controller using Proportional-Integral (PI) control is also evaluated in terms of its ability to maintain the operation at the generated set-point and to achieve the target CSD.

2. Extension of Analytical CSD Estimator

Previously, the original analytical CSD estimator for one-dimensional crystallisation process has been developed by Nagy and Aamir (2012) which incorporating the growth kinetics without considering the effects of agglomeration and breakage phenomena. In this work, the original analytical CSD estimator has been extended to cover the effects of agglomeration and breakage as well as agitation factor in the case of size independent growth rate for assessing its influence on the performance of the final CSD. The extension of analytical CSD estimator to cover the effects of agglomeration and breakage are shown in Table 1. Here the both agglomeration and breakage are represented as kinetic power law equation and the kinetic equation is the function of supersaturation, total crystal mass and agitation. This kinetic equation is taking account the overall effects of both phenomena and neglecting the effects of individual phenomena (Quintana-hernandez et al., 2004). The function of this estimator is to generate a supersaturation set-point and total batch crystallisation time that gives a target CSD by specifying the initial seed of CSD, the target CSD, the agglomeration-breakage and growth kinetics. It is based on the assumptions of constant supersaturation throughout the entire crystallisation process.

Table 1: Extended Analytical CSD estimator

Characteristic	Analytical model equations
Size independent growth: $G = K_g S^g N_{rpm}^q$	Final CSD: $f_{n,i} = f_{n0,i} + \alpha,\ i = 1, 2, \ldots . N$ where $\alpha = K_a S^a M_c^k N_{rpm}^r$
	Final characteristic length: $L_{x,i} = L_{x0,i} + K_g S^g N_{rpm}^q t_c,\ i = 1,2, \ldots . N$

To generate the optimal supersaturation set-point using the extended analytical CSD estimator, three conditions must be taken into accounts which are the initial seed of crystals, a target CSD and a model that represents the growth and agglomeration-breakage kinetics must be available. Usually, the target CSD, one or two dimensional function $f_{n,l\ target}$ is supplied in the form of normal, lognormal or bimodal distribution (Samad et al., 2013). In this work the initial seed distribution of the seeded batch crystalliser is assumed to be a parabolic distribution in the range of 250 to 300 μm as shown in Eq(1). The initial seed of CSD needs to be specified since it is serves as a starting point for the crystals starts to grow from the initial characteristic length (Samad et al., 2013).

$$\begin{aligned} &n\ (L,0) = 0.0032\ x\ (300 - L)\ x\ (L - 250)\ ,\ \text{for } 250\ \mu m \le L \le 300\ \mu m \\ &n\ (L,0) = 0,\ \text{for } L < 250\ \mu m \text{ and } L > 300\ \mu m \end{aligned} \tag{1}$$

In this study, the target seed distribution chosen is also in the parabolic distribution as shown in the Eq(2). It is important to remark that although arbitrary target CSD can be chosen but the same distribution functions for initial seed and target CSD need to be used. The target CSD may not be attained if different distribution function is used for initial seed and target CSD.

$$\begin{aligned} &n\ (L,0) = 0.0035\ x\ (420 - L)\ x\ (L - 370)\ ,\ \text{for } 370\ \mu m \le L \le 420\ \mu m \\ &n\ (L,0) = 0,\ \text{for } L < 370\ \mu m \text{ and } L > 420\ \mu m \end{aligned} \tag{2}$$

Figure 1 shows the initial seed of CSD and target CSD generated from Eqs(1) and (2). Usually, in the case of size independent growth where the effects of both agglomeration and breakage are neglected, the peak and the curve shape of the initial and final CSD are similar except the mean of the characteristic length is increased due to the size independent growth effects (Samad et al., 2013). In this case study with the incorporation of agglomeration and breakage, both the curve shape of CSD and characteristic length are changed. The highest peak for the initial seed is 2 μm/g of solvent at mean characteristic length of 275 μm meanwhile for the target CSD is 2.12 μm/g of solvent at mean characteristic length of 395 μm.

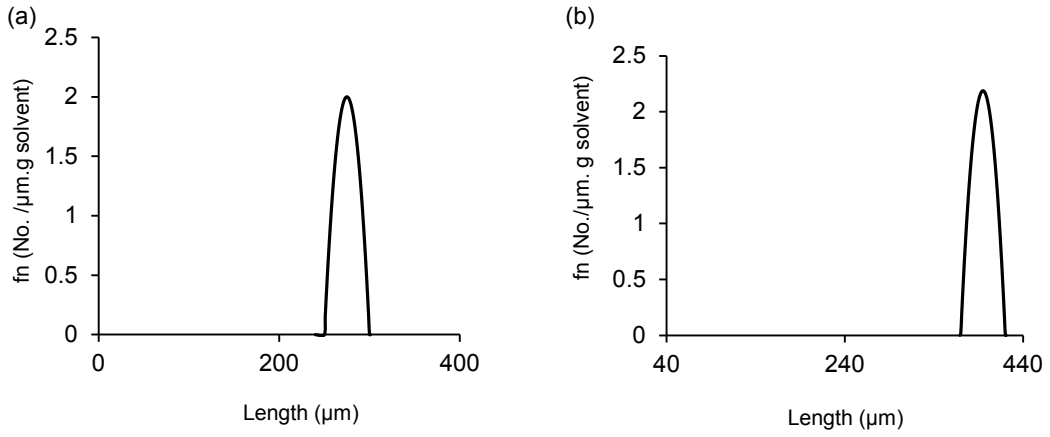

Figure 1: (a) Initial seed distribution and (b) target seed distribution for sucrose crystallisation

A model-based approach as shown in Eqs(3) to (6) is then used to optimise the supersaturation set point and the total crystallisation time in order to achieve the desired target CSD. The objective is to minimise the sum of squares of the relative errors between the desired target CSD and a predicted CSD obtained through the extension of analytical CSD estimator.
Minimise:

$$F_{obj} = \sum_{i=1}^{N} \frac{f_{n,i} - f_{n,i_{target}}}{f_{n,i_{target}}}^2 \quad (3)$$

Subject to: S_{sp}, t_c

$$S_{sp,min} \leq S_{sp} \leq S_{sp,max} \quad (4)$$

$$t_{min} \leq t_c \leq t_{max} \quad (5)$$

$$c_{t,batch} \leq c_{f,max} \quad (6)$$

Where N is the number of discretisation points, $f_{n,i}$ is the predicted CSD that is obtained from the analytical CSD estimator and $f_{n,i_{target}}$ is the desired target CSD, $c_{t,batch}$ is the expected solute concentration at the end of the batch and $c_{f,max}$ represents the maximum acceptable solute concentration at the end of the batch to achieve the required yield. The optimisation problem consisting of Eqs(3) to (6) is then constructed and is solved using a sequential quadratic programming (SQP) based solver to obtain the optimal set-point.

3. Application of the Extended Analytical CSD Estimator

The case study used to demonstrate the application of the extended analytical CSD estimator is highlighted through sucrose crystallisation process which has been adopted from Quintana-hernandez et al. (2004). The mathematical model used for sucrose case study is shown in Table 2 which is similar as published in the literature (Quintana-hernandez et al., 2004) but in this work the population balance equations are solved using the method of classes and the seed of the CSD is included as shown in Figure 1(a). Meanwhile Table 3 shows the values of all parameters and known variables used to solve the mathematical model shown in Table 2. In this work the sucrose crystallisation mathematical model is developed in MATLAB 2014a software and is solved using “ode15s” solver. Based on the specified initial seed and target CSD in Figure 1 as well as kinetic parameters in Table 3, the following optimal set-point generated from analytical estimator was obtained for achieving the desired target CSD where the supersaturation set-point is 0.0312 g sucrose per g water and the total crystallisation time is 180 min. In order to maintain the supersaturation at the generated set-point, a proportional integral (PI) controller is employed.

Table 2: List of model equations for the one-dimensional model for sucrose crystallisation (Quintana-hernandez et al., 2004)

Population balance equation	$\frac{dN_1}{dt} + \frac{G(L_1)}{2\Delta(Cl_2)}N_2 + \frac{G(L_1)-G(L_0)}{2\Delta(Cl_2)}N_1 = B + \alpha \quad , \quad i = 1$
(size independent growth)	$\frac{dN_i}{dt} + \frac{G}{2\Delta(Cl_i)}N_i - \frac{G}{2\Delta(Cl_{i-1})}N_{i-1} = \alpha \quad , \quad 1 \le i \le n$
	$\frac{dN_n}{dt} + \frac{G}{2\Delta(Cl_n)}N_n - \frac{G}{2\Delta(Cl_{n-1})}N_{n-1} = \alpha \quad , \quad i = n$
Overall mass balance (solute concentration)	$\frac{dc}{dt} = -3\rho_c k_v G\left(\sum_{i=1}^{3} S_{xi}^3 \frac{dN_i}{dt}\right)$
Energy balance	$\frac{dT}{dt} = -\frac{UA}{Mc_p}(T - T_w) - \frac{\Delta H}{c_p} 3\rho_c k_v G\left(\sum_{i=1}^{3} S_{xi}^3 \frac{dN_i}{dt}\right)$
Energy balance for cooling jacket	$\rho_w V_w c_{pw} \frac{dT_w}{dt} = \rho_w F_{win} c_{pw}(T_{win} - T_w) + U_1 A_1 (T - T_w) + U_2 A_2 (T_{ex} - T_w)$
Saturation concentration	$c^{sat}(T) = 6.29 \times 10^{-2} + 2.46 \times 10^{-3} T - 7.14 \times 10^{-6} T^2$
Supersaturation	$S = \frac{c - c^{sat}}{c^{sat}}$
Nucleation	$B = K_b S^b M_c^j N_{rpm}^p$
Crystal growth rate (length direction)	$G = K_g S^g N_{rpm}^q$
Characteristic size	$S_{xi} = \frac{L_{xi} - L_{xi-1}}{2}$
Production reduction-term	$\alpha = K_a S^a M_c^k N_{rpm}^r$
Total crystal mass	$M_c = \rho_c k_v \left(\sum_{i=1}^{3} S_{xi}^3 N_i\right)$
Cystal size distribution	$f_n(L_{xi}) = \frac{(N_i/\Delta cl_i) + (N_{i+1}/\Delta cl_{i+1})}{2}$

Table 3: Parameter values for sucrose crystallisation (Quintana-hernandez et al., 2004)

Parameter	Value	Units
Nucleation order, *b*	0.01	-
Kinetic coefficient for nucleation, K_b	85.70	No. of particles/cm^3.min.(g/cm^3)^j.(rpm)^p
Growth order, *g*	1.00	-
Kinetic coefficient for crystal growth, K_g	1.33 x 10^{-4}	cm/min.(rpm)^q
Kinetic coefficient for production-reduction, K_a	1.00	No. of particles/cm^3 magma.cm^2.min.(g/cm^3)^k.(rpm)^r
Production-reduction term, *a*	0.1	-
Mass order at nucleation, *j*	5.00 x 10^{-3}	-
Mass order at production-reduction, *k*	0.09	-
Agitation order at growth, *p*	0.05	-
Agitation order at growth, *q*	0.5	-
Agitation order at production-reduction, *r*	1.0 x 10^{-3}	-
Heat capacity of solution, C_{ps}	2.4687	J/g.°C
Density of crystals, ρ_c	1.588	g/cm^3
Magma volume, *V*	2,230	cm^3
Heat capacity of water, C_{pw}	4.18	J/g.°C
Volume of water, V_w	820	cm^3
Exterior temperature, T_{ex}	29	°C
Mass of total, M_T	3,328	g
Mass of water, M_w	800	g
Mass of solvent, M_s	2,528	g
Mean length, ΔL	20.2525	µm
Crystal length, L_o	15.126	µm
Volumetric shape factor, k_v	π/6	-
Initial temperature, T_o	70	°C
Density of water, ρ_w	1.0	g/cm^3

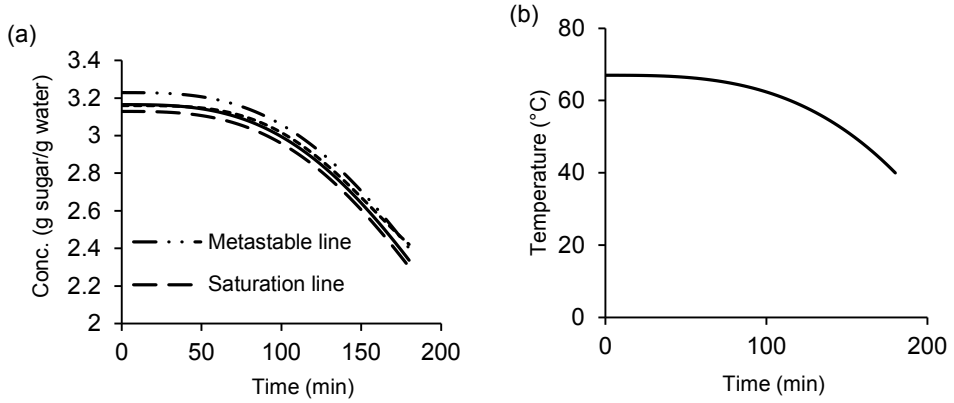

Figure 2: (a) Concentration profile of sugar in water (b) Temperature profile of sucrose

Based on the simulation results, Figure 2 shows the concentration profiles which lie between saturation line and metastable line and the temperature profiles when cooling down from 67 °C to 40 °C. A PI controller has been implemented to control the concentration at the set-point generated from the extended analytical CSD estimator. Based on the concentration profiles result, it can be concluded that the sucrose concentration was successfully maintained at the required set-point until the end of operation. The sucrose concentration initially at 3.16 g sucrose/g water is decreased steadily until 2.42 g sucrose/g water at the end of operation time of 180 min. The solubility line is temperature dependent. Since the sucrose concentration is decreasing, the solubility line must also decrease in order to maintain the operation at the desired set point profile (constant supersaturation), which results in a decrease of the temperatures.

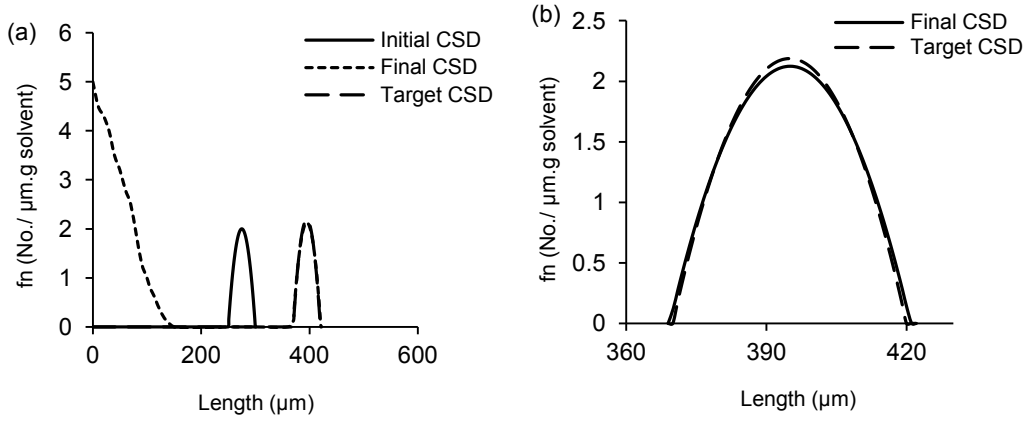

Figure 3: (a) Crystal size distributions (CSD) for sucrose (b) Close up of target and final CSD

Figure 3(a) shows the initial seed and final CSD for sucrose crystallisation process. When the agglomeration-breakage is implemented, the sucrose crystallisation resulted in final CSD is about 2.08 µm per g of solvent at the highest peak of CSD, with an approximate mean of 395 µm as similar to the targeted distribution. Initially the highest peak of the initial seed is 2 µm/g of solvent and it is clearly shows that the highest peak is increased at the final CSD. This increment is caused by the agglomeration-breakage kinetic which has been included in the sucrose crystallisation. It can be remark that the sucrose crystallisation operation in this study is influenced by agglomeration effects rather than breakage phenomena due to the increment of the highest peak of CSD (Samad et al., 2013). The initial seed originally at mean of 275 µm has been grown to the mean of 395 µm due to the size independent kinetic growth rate as shown in Figure 3(a). In addition, the secondary peak is also appeared in the final CSD due to the nucleation effects that cannot be captured by the analytical estimator. Figure 3(b) is the close up of target and final CSD. It is clearly shown that the final CSD has reach the target CSD in the end of the operation indicating the generated set-point from the extended analytical CSD estimator is indeed reliable and the PI controller successfully maintained the operation at the generated set-point to achieve the target CSD.

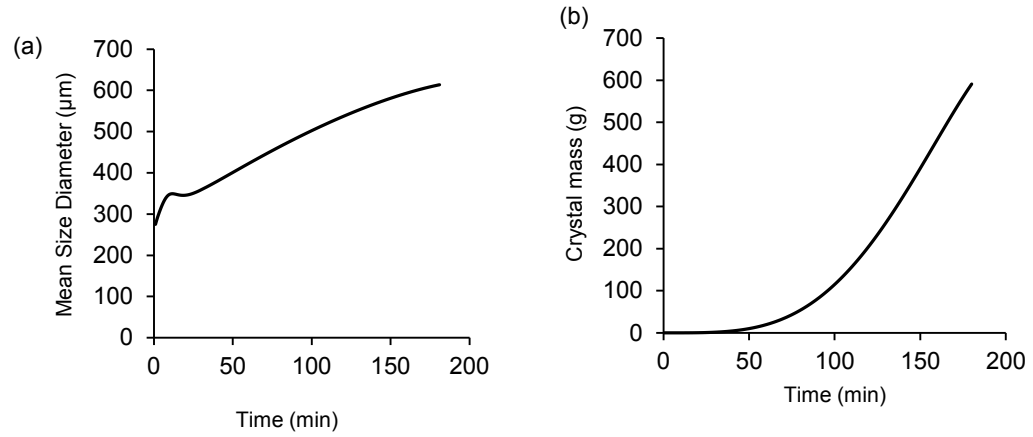

Figure 4: (a) Mean size diameter (b) Total crystal mass of sucrose crystallisation

Meanwhile Figure 4 shows the mean size diameter and total crystal mass for the sucrose crystallisation process. The initial mean size diameter for the seed crystals is 275 µm and the mean size is increased to 614 µm at the end of operation. Meanwhile the total mass of seed crystal is increased from 5 g to 590.79 g. This is due to the sucrose in the solution has been transferred into a seed crystal and thus resulting into the increment of the mean size diameter and the total crystal mass.

4. Conclusions

An extended analytical CSD estimator for all the necessary phenomena (crystal growth, agglomeration and breakage) has been developed in order to determine the set-point trajectory for the desired target CSD. Sucrose in batch cooling crystallisation process was considered as a case study. It was found that the implementation of agglomeration and breakage phenomena in an extended analytical estimator to generate set-points is applicable and the controller is successfully maintained the operation at the generated set-points and the target CSD is also achieved.

Acknowledgments

The financial support for this Master project provided by the Universiti Malaysia Pahang (UMP) Vot Number RDU140395 is gratefully acknowledged.

References

Cristofer B.B., Hernandez J.G.S., Hernandez S., Antonio C.G., Ramirez A.B., 2011, Design and optimization of a hybrid distillation/melt crystallization process using genetic algorithms, Chemical Engineering Transactions 24, 427-432.

Ghadipasha N., Baratti R., Tronci S., Romagnoli J.A., 2015, A deterministic formulation and on-line monitoring technique for the measurement of salt concentration in non-isothermal anti-solvent crystallization processes, Chemical Engineering Transactions 43, 1375-1380.

Nagy Z.K., Aamir E., 2012, Systematic design of supersaturation controlled crystallization processes for shaping the crystal size distribution using an analytical estimator, Chemical Engineering Science 84, 656-670.

Nagy Z.K., Braatz R.D., 2012, Advances and new directions in crystallization control, Annual Review of Chemical Biomolecular Engineering 3, 55-75.

Quintana-Hernandez P., Bolanos-Reynoso E., Miranda-Castro B., Salcedo-Estrada L., 2004, Mathematical modelling and kinetic parameter estimation in batch crystallization, American Institute of Chemical Engineers 50 (7), 1407-1417.

Samad N.A.F.A., Sin G., Gernaey K.V., Gani R., 2013, A systematic framework for design of process monitoring and control (PAT) systems for crystallization processes, Computers and Chemical Engineering 54, 8-23.

Vetter T., Burcham C.L., Doherty M.F., 2014, Regions of attainable particle sizes in continuous and batch crystallization process, Chemical Engineering Science 106, 167-180.